

COMMUNICATION

Ferromagnetism induced by in-plane strain in a bulk VS₂ based superlattice: (LiOH)_{0.1}VS₂

Ruijin Sun,^{*a} Jun Deng,^b Yuxin Ma,^b Munan Hao,^b Xu Chen,^b Dezhong Meng,^a Changchun Zhao,^a Shixuan Du,^b Shifeng Jin,^{*b} and Xiaolong Chen^{*b}

a. School of Science, China University of Geosciences, Beijing (CUGB), Beijing, 100083, China.

b. Institute of Physics, Chinese Academy of Science, Beijing, 100190, China.

E-Mail: srj@cugb.edu.cn

Experimental and Methods Section

Sample synthesis.

K_xVS₂ Crystal: V and S powder were ground with a reactive flux K₂S₂. The molar ratio of K₂S₂:V:S was kept constant at about 0.5: 1: 1. After all the starting materials were thoroughly mixed, they were loaded into a Al₂O₃ crucible and then sealed in a quartz tube. The quartz tube was placed in a muffle furnace, the furnace was heated at a rate of 20 degree/min to 1050 °C, then kept at 1050 °C for 5 hours, and then cooled to 550 °C at a rate of 3-10 °C/hour. Following natural cooling to room temperature, silver needle-like single crystal K_xVS₂ was obtained.

1T-VS₂ Crystal: K_xVS₂ crystals and deionized water were placed in a 25-mL Teflon-lined autoclave with 60% of its capacity. The autoclave was then tightly closed and heated at 140 °C for 7 days, the silver 1T-VS₂ crystals were filtered after washing with deionized water.

(LiOH)_{0.1}VS₂ Crystal: K_xVS₂ crystals and 2g LiOH·H₂O were placed in a 25-mL Teflon-lined autoclave filled 60% of its capacity with deionized water. The autoclave was then tightly closed and heated at 140 °C for 7 days, the silver (LiOH)_{0.1}VS₂ crystals were filtered after washing with deionized water.

Characterization

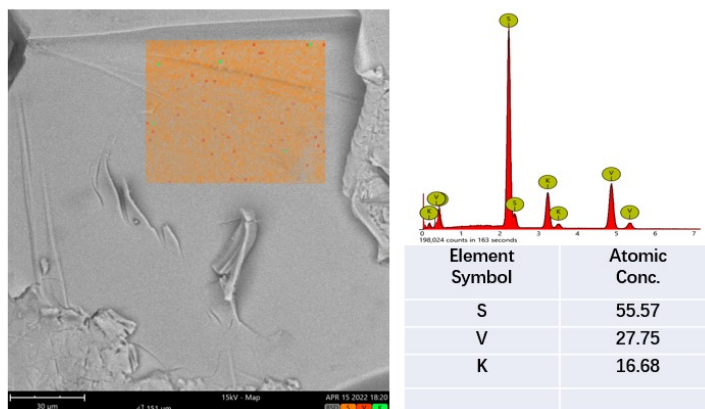
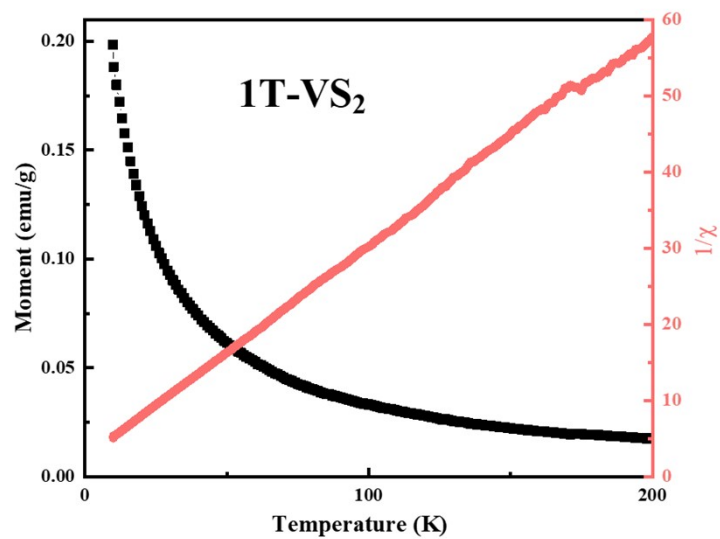
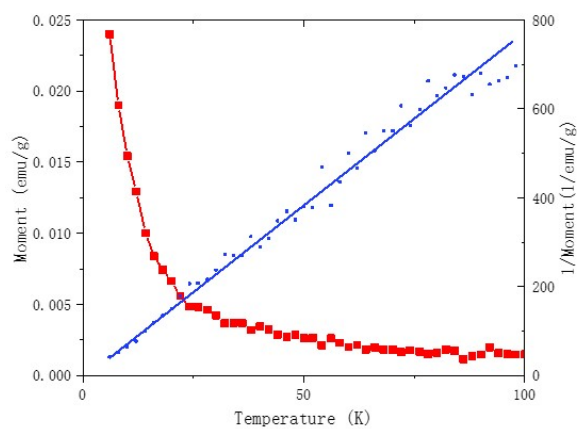
Powder X-ray diffraction (PXRD) patterns were collected at room temperature on a Rigaku smart Lab X-ray diffractometer operated at 40 kV voltage and 40 mA current using Cu K α radiation ($\lambda=1.5406\text{\AA}$). The 2θ range was 10–80° with a step size of 0.01. Indexing and Rietveld refinement were performed using the DICVOL91, Fullprof, and MDI Jade programs. Single crystal X-ray diffraction (SCXRD) patterns at 295 K were collected using a Bruker D8 VENTURE PHOTO II diffractometer with multilayer mirror monochromatized Mo K α ($\lambda = 0.71073\text{\AA}$) radiation. Unit cell refinement and data merging were performed using the SAINT program, and an absorption correction was applied using Multi-Scans scanning. Structural solutions were obtained by intrinsic phasing methods using the program APEX3, and the final refinement was completed with the Jana 2020 suite of programs. The electron density maps of the two samples were firstly constructed by the charge flipping method implemented in the Jana2020 software. Scanning electron microscopy (SEM) images were taken on a Phenom pro XL microscope equipped with an electron microprobe analyzer for the semiquantitative elemental analysis in the energy-dispersive X-ray spectroscopy (EDS) mode.

The density functional theory (DFT) calculations

The density functional theory (DFT) calculations were performed within the Vienna ab initio simulation packageⁱ. We adopted the generalized gradient approximation (GGA) in the form of Perdew-Burke-Ernzerhof (PBE) for the exchange-correlation potentialsⁱⁱ. The projector augmented-wave (PAW) pseudopotentials were used with a plane wave energy of 500 eV; $3p^63d^44s^1$ for V, and $3s^23p^4$ for S electron configuration were treated as valence electrons. The van der Waals interaction was considered using DFT-D3 method of Grimme. The GGA+*U* method with Dudarev's approach was applied to V-*d* orbitals, where the effective *U* parameter $U_{\text{eff}} = U - J$ was set as 1 eV. A Monkhorst-Packⁱⁱⁱ Brillouin zone sampling grid with a resolution of $0.02 \times 2\pi\text{\AA}^{-1}$ was used. The self-consistent field procedure was considered convergent when the energy difference between two consecutive cycles was lower than 10^{-6} eV. The lattice constants and atomic coordinates were relaxed until all the forces on the ions were less than 0.01 eV/Å. For (LiOH)_{0.1}VS₂, LiOH were omitted, and the

lattice constant were kept constant during the relaxation, which were derived from the experimental results. In calculating magnetic anisotropy energy calculation, a cutoff energy of 700 eV and a denser kspacing of $0.01 \times 2\pi \text{ \AA}^{-1}$ were adopted. And the energy difference between two consecutive cycles in the self-consistent calculation was improved to 10^{-8} eV.

Figure Section

Fig. S1 SEM image and EDS compositional mapping of $K_{0.6}VS_2$.Fig. S2 FC curves obtained with an out-of-plane magnetic field of 1 T for $(LiOH)_{0.1}VS_2$.Fig. S3 FC curves obtained with an out-of-plane magnetic field of 1 T for $K_{0.6}VS_2$.

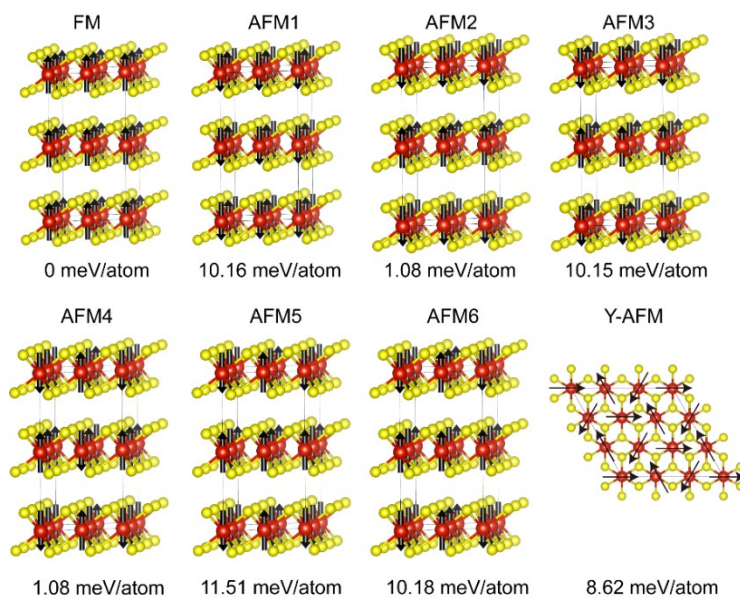
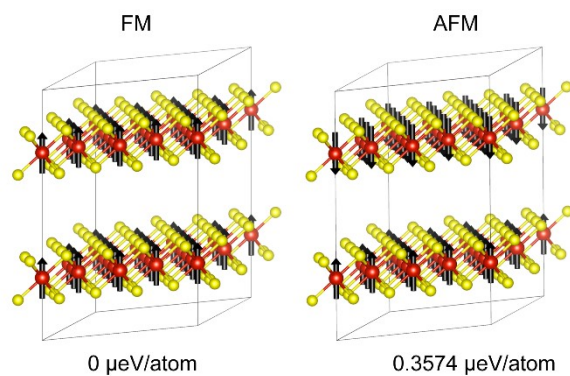
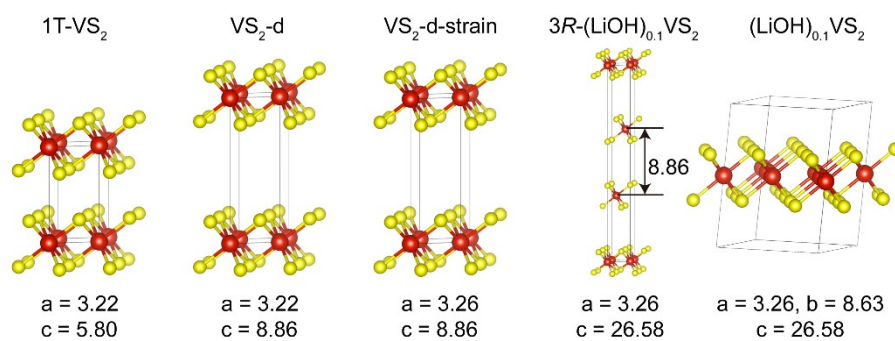
Fig. S4 The formation energy of different magnetic states in bulk 1T-VS₂.Fig. S5 The formation energy of different magnetic states in (LiOH)_{0.1}VS₂.

Fig. S6 The definition of the structures used in DFT calculations.

Table Section

Table S1. Molar ratio for Li, V, S via ICP-AES method.

Element	Li	V	S
Molar ration	0.11	0.96	2

Table S2. Crystallographic data of (LiOH)_{0.1}VS₂.

Formula	S10 V4.92 O 0.484 Li 0.476
Formula Weight	575.95
Space group	<i>P</i> - 1
a, c(Å)	5.6557(6), 8.6279(2), 9.0551(7)
Z	1
Crystal size(μm ³)	87 * 64 * 23
Temperature(K)	298
Radiation(Å)	Mo-Kα λ = 0.71073
R ₁ , wR ₂ , S	0.0671, 0.1544, 1.1000

Atomic positions and equivalent displacement parameters

Atom	Mult.	x	y	z	Occ.	U _{iso}
V1	2	0.2013(4)	0.6001(3)	0.4997(3)	0.99(2)	0.0238(3)
V2	2	-0.3989(3)	0.8002(2)	0.49931(19)	0.98(7)	0.0240(5)
V3	1	0	1	0.5	0.98(3)	0.0240(6)
S1	2	0.4782(4)	0.4326(3)	0.3362(3)	1	0.0181(5)
S2	2	-0.3217(4)	1.0331(3)	0.3359(3)	1	0.0184(5)
S3	2	-0.0775(4)	0.7665(3)	0.6644(3)	1	0.0177(5)
S4	2	-0.1217(4)	0.6330(3)	0.3356(3)	1	0.0163(5)
S5	2	0.2785(4)	0.8329(3)	0.3362(3)	1	0.0183(5)
O1	2	0.2519(2)	0.7004(8)	-0.0233(5)	0.242(3)	0.059(3)
Li	2	0.7116(3)	0.6118(6)	0.0023(1)	0.238(6)	0.068(2)

Table S3. Selected bond length and bond angle for (LiOH)_{0.1}VS₂, 1T-VS₂ (PDF card- 04-003-2308) and LiOH (PDF card- 00-032-0564).

	(LiOH) _{0.1} VS ₂	1T-VS ₂	LiOH
Bond length (Å)			
V-S	2.375(3)	2.34986(1)	----
Li-O	2.481(3)	----	2.01296(6)
Bond angle (deg)			
S-V-S	86.39(9)	86.4274(0)	----

-
- i. Kresse, G., Furthmuller, J., Efficiency of ab-initio total energy calculations for metals and semiconductors using a plane-wave basis set. *Comput. Mater. Sci.* **6** (1), 15-50 (1996).
 - ii. Perdew, JP., Burke, K., Ernzerhof, M., Generalized gradient approximation made simple. *Phys. Rev. Lett.* **77**, 3865-3868 (1996).
 - iii. Monkhorst, H. J., Pack, J. D., Special points for brillouin-zone integrations. *Phys. Rev. B* **13**, 5188-5192 (1976).